nature climate change

SUPPLEMENTARY INFORMATION

DOI: 10.1038/NCLIMATE1580

Different glacier status with atmospheric circulations in Tibetan Plateau and surroundings

Tandong Yao[1, 3,*], Lonnie Thompson[2, 1], Wei Yang[1], Wusheng Yu[1], Yang Gao[1], Xuejun Guo[1], Xiaoxin Yang[1], Huabiao Zhao[1], Keqin Duan[3, 1], Baiqing Xu[1], Jiancheng Pu[3], Anxin Lu[3,1], Dahe Qin[3], Yang Xiang[1], Dambaru B. Kattel[1], Daniel Joswiak[1]

[1]*Key Laboratory of Tibetan Environmental Changes and Land Surface Processes, Institute of Tibetan Plateau Research, Chinese Academy of Sciences, Beijing, 100101, China.*

[2]*Byrd Polar Research Center and School of Earth Sciences, Ohio State University, Columbus, OH 43210, USA.*

[3]*State Key Laboratory of Cryosphere Sciences, Chinese Academy of Sciences, Lanzhou 730000, China.*

*corresponding author:

Email: tdyao@itpcas.ac.cn

4A Datun Rd., Chaoyang District, Beijing, P.R. China

Supporting Online Material

Glacial area in the Tibetan Plateau (TP) and surroundings is still an issue to be precisely inventoried. Here we provide a figure of ~100, 000 km^2 in Table S1 based on studies of Yao et al.[1] and Dyurgerov[32].

There are many publications in Chinese journals about glacial fluctuations in China[33-50]. Those studies showed different pictures of glacier fluctuations. Some indicated heterogeneous retreat magnitudes in different areas, with the largest retreat in the margin of the TP and decreasing to the interior[33-43], while others showed a few advancing glaciers in the southeastern TP and central Himalayas[46-47]. However, Jin et al.[47] admitted, from their own experiences, that the 'advancing glaciers' might be misled by satellite images with heavy snow and shadow. Two advancing glaciers interpreted from early satellite images in the paper of Liu et al.[46] are also retreating glaciers according to more reliable satellite images. Some studies emphasized the unique response of debris-covered glaciers to climate changes[15,51, 52]. A few studies of in situ observation of glacial length and mass balance do exist[53,54], but are too sparse to shed light on a holistic picture of glacial fluctuations of the region. Recently some more data are published in the southern TP and Himalayas using new technologies and methods[52]. The situation thus underlines the necessity for a comprehensive study of glacial area based on satellite images and in situ glacial length and glacial mass balance. This is the major purpose of our study in this paper.

1. Glacier area reduction

Glacier area change is studied using remote sensing images and topographic maps. Among the glacial area analysis of 16 river basins in seven regions, nine are based on literatures and seven are based on our studies (four had not been published). It's important to evaluate its potential uncertainty. The accuracy of glacier delineation based on remote sensing images depends on the resolution of the utilized image, the conditions at the time of the acquisition (especially seasonal snow) and the knowledge of the operator to decide the lake region, glacier in cast shadow, perennial or seasonal snow, debris-covered area and location of ice divides and might be subjective[55]. The mapping uncertainty of our studies is less than 3% for clean-ice glaciers and 4% for debris-covered glaciers in the Boshula Mountain Range, Southeastern Tibet, Koshi River Basin Nepal, Mapam Yumco Basin, Geladandong and Shulenan Mountain. This is similar with previous studies, which reported a mapping uncertainty of ±2-3% for clean-ice glacier[56,57], of ±3-4% for debris-covered glacier for ASTER, Landsat TM by comparison with other high-resolution images or estimation[58]. However, it's difficult to evaluate the uncertainty of the result from previous studies (cited in this study), since they were from different operators using different methods. To reduce large uncertainty, we only use the results of the studies with similar resolution images (Landsat or ASTER) and at the end of snow season. The uncertainty is no more than 5%.

There are totally 7,090 glaciers (~13,363.5 km^2) analyzed for glacial area reduction in this study. We have measured 2,135 glaciers (~3154.5 km^2) based on digitized glacier inventories from topographic maps and remote sensing images in six river basins in the TP and surroundings. The other 4,955 glaciers (~10209.0 km^2) were summarized from the results of previous studies[59-69].

The locations of studied glaciers for area reduction are shown in Figure S1 and Table S2. The total glacier area of 7,090 glaciers has decreased from 13,363.5 km^2 to 12,130.7 km^2 in the period between the 1970s and 2000s. The average decreasing rate is ~-0.30% a^{-1} for the TP and surroundings, but different from region to region, with the largest (-0.57% a^{-1}) in Region I and the smallest (-0.07% a^{-1}) in Region V (Table S3).

We have also compared retreat magnitude of different glacier sizes in different regions. Figure S2 summarized the change of glacial area with different sizes in different regions. According to the sizes, glaciers were classified into four types: <1km^2, 1.0-5.0 km^2, 5.0-10.0 km^2 and >10km^2. Although the change rate of smaller glaciers is larger than that of larger glaciers in all the regions, the general pattern of glacial retreat is controlled by regional climate. In a region with the same climate dominance, such as monsoon or westerlies, glaciers undergo similar retreat tendency, no matter what sizes the glaciers are.

2. Glacial length fluctuation

We have analyzed glacial length fluctuation of 82 glaciers from the 1970s to 2000s. Among them, the length fluctuation of 13 glaciers is based on our *in situ* observations and that of the other 69 is summarized from previous studies[70-89]. The general pattern of glacial length fluctuation shows more intensive retreat in the

Himalayas, with largest retreat of three glaciers in the southeastern TP or the eastern Himalayas and moderate retreat of eight glaciers in the central Himalayas and 20 glaciers in the western Himalayas, and decreasing retreat of five glaciers in the interior northeastern TP and five glaciers in the Nyainqentanglha Mountain, and stable or even advancing characteristics in the eastern Pamir regions and west Kunlun Mountains (among the 41 glaciers, 17 retreated and 10 were stable, while 14 advanced).

3．Glacial mass balance change

3.1 Current status of glacial mass balance

We have analyzed 15 glaciers to assess the current mass balance status in the TP and surroundings (Table S6-S7). Among them, 11 glaciers are based on our *in situ* measurements and the other four are summarized from previous studies[90-92]. The results of the 11 glaciers are presented in the following:

The Parlung No.10 Glacier

The Parlung No.10 Glacier (29º17´N, 96º54´E) is a valley glacier (Figure S3a) flowing from 4,900 to 5,625 m, with an area of 2.1 km^2 and a length of 3.5 km. A total of 11 measuring stakes have been distributed on this glacier. Figure S3c shows the significant variations of spatial distribution of net mass balance year by year, accompanied with ELAs fluctuations (Figure S3b) (data for 2009/10 is absent due to measuring stakes falling down). 2008/09 is the most negative mass balance year we have measured, shown both by the spatial distribution of net balance (negative almost on the whole glacier, shown in Figure S3c and Table S7) and ELA (Figure S3b). The ELAs in the past four years have shifted from 5,419m to 5,500m, and nearly reached the glacier summit in 2008/09.

The Parlung No.12 Glacier

The Parlung No.12 Glacier (29º18´N, 96º54´E) is a small cirque glacier with an area of about 0.2 km^2 and a length of nearly 0.6 km (Figure S4a). Its elevation ranges from 5,130 to 5,265 m. A total of 5 measuring stakes have been distributed on this glacier. The spatial distribution of net balance demonstrates negative net balance on the whole glacier every year (Figure S4c) and the ELAs have already risen beyond the glacier summit during the period of measurement. This glacier is now suffering from significant mass deficit.

The Parlung No.94 Glacier

The Parlung No.94 Glacier (29º23´N, 96º59´E) is a valley glacier with an area of 2.5 km^2, a length of 2.9 km and its elevation range from 5,000 to 5,635 m (Figure S5a). A total of 19 measuring stakes have been spatially distributed on this glacier. With similar glacier area and altitudinal range, both the spatial distribution of net balance and ELAs variations show a similar pattern with the Parlung No.10 Glacier (Figures S5b-c). The most negative mass balance with the highest ELA occurs in 2008/09.

The Parlung No.390 Glacier

The Parlung No.390 Glacier (29º21´N, 97º01´E) flows from an elevation of 5,160 to 5,460 m, with an area of about 0.5 km^2 and a length of 1.2 km (Figure S6a). A total of 5 measuring stakes have been distributed along the central axis of this glacier. Located in the same region with the Parlung No.10, 12 and 94 Glacier, the spatial distribution of net balance and ELAs of the Parlung No.390 Glacier also show a similar pattern (Figures S6b-c).

The Gurenhekou Glacier

The Gurenhekou Glacier (30°11′N, 90° 28′E, area 1.4 km^2, length 2.9 km) lies near the town of Yangbajin on the southern slope of Nyainqentanglha Mountain. The glacier ranges from 6,040 to 5,525 m in elevation (Figure S7a). A total of 12 measuring stakes have been spatially distributed on this glacier. Different from the four glaciers in the southeastern TP, the circumstance of spatial distribution of negative net balance on the whole glacier did not occur on the Gurenhekou Glacier. In contrast, the mass balance is positive(Figure S7c) with descending ELA (Figure S7b) in 2007/08.

The Zhongxi Glacier

The Zhongxi Glacier (30°52′N, 91°27′E, area 1.6 km^2, length 2.6 km) lies on the northeastern Nyainqentanglha Mountain Range, near the Npen Co lake (Figure S8a). The elevations of the glacier summit and terminus are 6,210 and 5,376 m, respectively. A total of 16 measuring stakes have been spatially distributed on this glacier. The three-year measurements of this glacier show a similar pattern of spatial distribution of net balance and ELA with the Gurenhekou Glacier. Slight positive mass balance occurred in 2007/08 (Figures S8b-c).

The Kangwure Glacier

The Kangwure Glacier (28°28′N 85°49′E, area 1.9 km^2, length 3.1 km) lies on the northern slope of central Himalayas range, near the Xixiabangma Mountain (Figure S9a). The glacier ranges from 6,060 to 5,690 m. A total of 16 measuring stakes have been spatially distributed on this glacier. Due to lack of mass balance measurement in 2006, we take the average between 2005/06 and 2006/07 for 2005/06 and 2006/07, respectively. The data in 2007/08 is absent due to measuring stakes falling down. Located in the northern slope of Himalayas, the spatial distribution of net balance and ELAs show intensive mass loss (Figure S9b, 9c) although the average elevation of this glacier is very high. The spatial distribution of net balance is negative on the whole glaciers in 2005/07.

The Naimona'nyi Glacier

The Naimona'nyi Glacier (30º27´N, 81º20´E) is located in the northern slope of west Himalayas and is a valley glacier with an area of 7.8 km^2 and a length of 7.7 km (Figure S10a). Its altitudinal range is between 5,465 and 7,520 m. 16 measuring stakes have been spatially distributed on this glacier. Due to lack of measurement in 2006, we take the average between 2005/06 and 2006/07 for 2005/06 and 2006/07, respectively. This glacier suffers from significant mass deficit, with particular circumstance of negative net balance on the whole glacier between 2005/06 and 2006/07 (Figure S10c). An earlier study indicated that the glacier deficit status may have lasted for a long time[93].

The Muztag Ata Glacier

The Muztag Ata Glacier (38º14´N, 75º03´E) is located in West Kunlun Mountain. This glacier has an area of 0.96 km^2, with a length of 1.8 km (Figure S11a). Its altitudinal range is between 5,235 and 5,940 m. A total of 13 measuring stakes have been spatially distributed on this glacier. Due to lack of measurement in 2009, we take the average between 2008/09 and 2009/10 for 2008/09 and 2009/10, respectively. The spatial distributions of net balance are positive almost on the whole glacier during the period, except in 2002/03 (Figure S11c).

The Xiaodongkemadi Glacier

The Xiaodongkemadi Glacier (33°04´N, 92°05´E) is located at the headwaters of the Dongkemadi river, a tributary at the upper reaches of the Buqu River near the Tanggula pass. The Glacier is 1.8 km^2 in area, with a length of 2.8 km (Figure S12a). The elevations of the summit and terminus of the glacier are 5,926 and 5,380 m, respectively. A total of 25 measuring stakes were set up on the glacier. The most significant phenomena of the Xiaodongkemadi Glacier is negative net balance in

2009/10 (-1,066 mm), which is higher than that in 2007/08 (-80 mm) and 2008/09 (-91mm) by one order (Figures S12b-c).

The Qiyi Glacier

The Qiyi Glacier (39°15´N, 97°45´E) is located on the northern slope of Qilian Mts. Its area is 2.87 km^2, with a length of 3.8 km (Figure S13a). Its altitudinal range is between 4,304 and 5,159 m. A total of 28 measuring stakes were set up on the glacier. Similar with the Xiaodongkemadi Glacier, the mass balance is much more negative (-648 mm) in 2009/10, comparing with that in 2007/08 (-105 mm) and 2008/09 (-74 mm).

Generally, all the 11 glaciers show negative mass balance in the five years of measurement, except the Muztag Ata Glacier that shows positive mass balance in the past four years (Table S7). The most negative mass balance is observed in the southeastern TP, while positive mass balance is observed in the eastern Pamir regions.

3.2. Long-time series of mass balance

There are three glaciers with mass balance starting from the early 1990s or earlier. The Xiaodongkemadi Glacier has been continuously measured for mass balance starting from 1988/89. Otherwise, the Qiyi and Kangwure Glaciers have ten-year and two-year, respectively, *in situ* measurements before 2005. We have reconstructed the past mass balance using the relationship between the measured mass balance and meteorological data (Table S8). For the Qiyi Glacier, the *in situ* mass balance measurement first started in 1974/75 and measured discontinuously since. Wang et al (2010)[94] established a statistical model between ELAs and meteorological factors (warm air temperature and cold-season precipitation) on the basis of measurement of the ELAs. The reconstructed ELAs agreed well with the measured data. In this study, based on this model, we have reconstructed annual mass balances (B_n) in the Qiyi Glacier (B_n =11456-2.44×ELA, n=12, R^2=0.92). Figure S14 shows the comparison between the simulated annual mass balances with *in situ* measurements. The simulated mass balance agrees well with the measurements.

For the Kangwure Glacier, we have used mass balance data of 1991/92 and 1992/93[95], and that between 2005/06 and 2009/10. We used the meteorological data at Dingri meteorological station (about 100 km away from the Kangwure Glacier) to analyze the relationship between mass balance and meteorological factors. A regression model was used to reconstruct the mass balance since 1991/92 based on the meteorological factors (annual air temperature (T) and precipitation (P)) and 5-year *in situ* mass balance observations (the linear regression is B_n = -350×T+2.36×P-22.4, n=5, R^2=0.61) (Figure S15). The reconstructed mass balance data are shown in Table S8.

3.3 Climate controls over glacial mass balance

We've studied glacial mass balance of 11 glaciers on the TP. Mass balance measurement of glaciers with different sizes under different climate regimes demonstrates heterogeneous mass loss as shown in Figure S16. In the monsoonal region where precipitation is decreasing, glacial mass balance is the most negative. In contrast, in the westerly region where precipitation is increasing, glacial mass balance is positive. Glacial mass balance is moderate in the transitional region.

4. Contrast precipitation trends between Himalayas and Pamir regions

It was first proposed by Yao et al.[96], and Liu and Chen[23] that the amplitude of temperature change increases with elevations. Latest study by Frauenfeld et al.[97], Qin et al.[24], Kang et al. [54] and You et al. [98] found that, the TP is warming, and the warming rate increases with elevation before becoming quite stable with a slight decline near the highest elevations. However, by examining Figure 4 in Qin et al.[24], we found that the warming rate is most intensive between 4,800 and 6,200 m a.s.l, which covers the ablation area of almost all glaciers in the TP. This is still not conclusive, and more studies are necessary to narrow down the uncertainties before a definite conclusion is drawn.

Precipitation is a very important factor contributing to the glacial mass balance change. This is particularly the case in the TP and surroundings. The most intensive glacial shrinkage in the Himalayas coincides with the decreasing precipitation accompanied by the weakening Indian monsoon and the least intensive glacial shrinkage in the eastern Pamir regions is linking with the increasing precipitation accompanied by the strengthening westerlies (Figure 4 in the Text). The trends of decreasing precipitation in the Himalayas and increasing precipitation in the eastern Pamir regions are further supported by the Global Precipitation Climatology Project (GPCP) dataset[99] for the period 1979−2010. The precipitation series in the four grids numbered as 1-4 in Figure 4a in the eastern Pamir regions show statistically significant increasing trends at the 99% confidence level using the Mann-Kendall test (Figure S17). The precipitation series numbered as 5-8 and 14-16 in Figure 4a in the Himalayas exhibit statistically significant decreasing trends at the 99% confidence level (Figure S18). The series numbered as 9-13 are not as significant as those of 5-8 and 14-16, but still show obvious decreasing trends.

Figure S19 shows the seasonality of the precipitation at Linzhi, Bomi and Zayu stations in the Indian monsoon-dominated Himalayas and at Taxkorgen station in the westerlies-dominated Pamir regions, indicating strong seasonality characterized by high precipitation in the summer and low precipitation in the winter. Figure S20 shows the spatial features of GPCP seasonal precipitation trend in the summer and winter during 1979-2010. The results show a similar spatial pattern of the seasonal precipitation to that of annual precipitation (Figure 4a) in the text, demonstrating decreasing precipitation in the eastern Himalayas and increasing precipitation in the eastern Pamir regions. The decreasing trend is more intensive in the summer in the Indian monsoon-dominated Himalayas (Figure S20a), confirming the weakening Indian monsoon; while the increasing trend is more intensive in the winter in the westerlies-dominated Pamir regions (Figure S20b), confirming the strengthening westerlies.

Supplementary Tables

Supplementary Table S1. Distribution of Glaciers in the TP and surroundings calculated from Yao et al[1] and Dyurgerov[32]

Region	**Glacier area (km^2)**
Pamir	12,260
Qilian	1,931
Kunlun	12,267
Karakoram	16,600
Qiangtang Plateau	2,581
Tanggula	2,213
Gangdise	1,760
Nyainqingtanglha	9,120
Hengduan	1,579
Himalayas	33,050
Gindukush	3,200
Hinduradash	2,700
Total	**99,261**

Supplementary Table S2.Data and method for analyzing glacial area reduction in each basin

Studied regions	Basin	Periods	Data 1970s	Data 2000s	Methods
I	Boshula Mountain Range*	1975-2001	Topographic Map	ALOS AVNIR-2	Manual Delineation (MD)
	Southeastern Tibet*	1980-2001	Topographic Map/Landsat TM	Landsat ETM +/ASTER GDEM	Band ratio TM3/TM5, TM4/TM5 & Manual Adjustment (MA)
II	Nam Co Basin* [59]	1976-2001	Hexangon KH-9/ Landsat MSS	Landsat ETM+ / Terra ASTER	Band ratio TM3/TM5 & MA
	Southeast of West Nyainqentanglha[60]	1970-2000	Aerial Photography	Landsat ETM+	MD
III	Mt.Qomolangma National Nature Preserve[61]	1976-2006	Topographic map/Landsat MSS	Landsat TM/ ASTER GDEM	NDSI&NDWI&MA
	Koshi Basin Nepal*	1976-2000	Topographic map/Landsat MSS	Landsat ETM+/USGS SRTM	Band ratio TM3/TM5, TM4/TM5 & MA
IV	Mapam Yumco Basin* [62]	1974-2003	Topographic map	Landsat ETM+ / Terra ASTER	MD
	Naimona'Nyi Region[63]	1976-2003	Topographic Map/Landsat MSS	Landsat ETM+ / Terra ASTER	Supervised classification & MA
	Himachal Pradesh[64]	1962-2001	Topographic map	LISS-III/LISS-IV	MD
V	Muztag Ata[65]	1965-2001	Topographic Map	Terra ASTER	MD
	Yurungkax River[66]	1970-2001	Aerial Photography	Landsat ETM +	NDSI&MD
	Karamilan-Keriya River[67]	1970-1999	Topographic Map	Landsat ETM +	MD & Band ratio TM3/TM5
VI	Dongkemadi Region[68]	1969-2001	Aerial Photography	Landsat ETM +	MD
	Geladandong*	1969-2000	Aerial Photography/ Topographic map	Landsat TM	MD
	Xinqingfeng Ice Cap[69]	1971-2000	Aerial Photography	Landsat ETM +	MD
VII	Shulenan Mountain*	1970-1999	Topographic map	Landsat ETM +	MD

Note: * represent our studies.

Supplementary Table S3. Glacial area reduction during the past three decades from remote sensing images in the TP and surroundings

Studied regions	Basin	Periods	1970s Total number	1970s Total area (km^2)	2000s Total number	2000s Total area (km^2)	Total Area Change (km^2)	Percentage of Annual Area Change (%/y)	Regional Number	Regional Average (%/y)
	Boshula Mountain Range*	1975-2001	150	167.5	150	155.0	-12.5	-0.276		
I	Southeastern Tibet*	1980-2001	129	217.9	154	174.6	-43.3	-0.903	279	-0.57
	Nam Co Basin*[59]	1976-2001	305	212.5	305	198.1	-14.4	-0.261		
II	Southeast of West Nyainqentanglha[60]	1970-2000	612	682.4	612	646.6	-35.8	-0.169	917	-0.20
	Mt.Qomolangma National Nature Preserve[61]	1976-2006	2196	3212.1	2196	2710.2	-501.9	-0.504		
III	Koshi Basin Nepal*	1976-2000	840	1121.6	840	1079.3	-42.3	-0.151	3036	-0.41
	Mapam Yumco Basin*[62]	1974-2003	242	107.4	242	100.1	-7.3	-0.227		
IV	Naimona'Nyi Region[63]	1976-2003	98	87.0	98	79.4	-7.6	-0.312		
	Himachal Pradesh[64]	1962-2001	466	2077.0	466	1628.0	-449	-0.540	806	-0.42
	Muztag Ata[65]	1965-2001	128	377.2	128	373.0	-4.2	-0.030		
V	Yurungkax River[66]	1970-2001	372	1777.0	365	1772.0	-5	-0.009		
	Karamilan-Keriya River[67]	1970-1999	895	1374.2	890	1334.9	-39.3	-0.095	1395	-0.07
	Dongkemadi Region[68]	1969-2001	124	179.4	124	167.4	-12	-0.203		
VI	Geladandong*	1969-2000	190	899.3	190	884.4	-14.9	-0.052		
	Xinqingfeng Ice Cap[69]	1971-2000	64	442.7	64	436.2	-6.5	-0.049	378	-0.10
VII	Shulenan Mountain*	1970-1999	279	428.3	279	391.5	-36.88	-0.287	279	-0.29
	Total		**7090**	**13363.5**	**7103**	**12130.7**	**-1232.88**		**7090**	**-0.30**

Note:* represent our studies. Regional average is calculated by $RA=\sum_{i=1}^{n} P\times(\frac{T}{R})$;RA is regional weighted average; P is the percentage of annual area change on each basin; T is number of glaciers on each basin in 1970s, R is number of regional glaciers in 1970s; n is the number of basins on each region.

Supplementary Table S4 Glacial length fluctuation in the TP and surroundings in the past three decades. * represent our studies.

Studied regions	Mountains	Glacial Number	Glaciers	Latitude (N)	Longitude (E)	Area (km^2)	Length (km)	Orientation	Location	Periods	Total change (m)	Annual change (m/a)	Regional average (m/a)
I	Southeast TP	1	Ata*	29°10´	96°48´	13.8	16.7	S	Southeast TP	1973-2005	-1795	-56.1	-48.2
		2	Parlung No.4*	29°14´	96°55´	11.7	8	N	Southeast TP	1980-2005	-406	-15.6	
		3	Yanong[70]	29°19´	96°42´	191	32.5	E/SE	Southeast TP	1980-2001	-1534	-73	
II	Nyainqentanglha	4	Lanong[71]	30°26´	90°34´	7.46	3.5	N	Nyainqentanglha Mt.	1970-2007	-401.7	-13.2	-16.3
		5	Panu[71]	30°23´	90°31´	12.92	8.4	SE	Nyainqentanglha Mt.	1970-1999	-179.6	-10.2	
		6	Xibu[71]	30°23´	90°36´	31.6	10.6	E	Nyainqentanglha Mt.	1970-1999	-1130.2	-39	
		7	Zhadang*	30°29´	90°39´	2	2.5	NW	Nyainqentanglha Mt.	1970-2007	-410.5	-10.8	
		8	Gurenhekou*	30°11´	90°27´	1.4	2.9	SE	Nyainqentanglha Mt.	1974-2004	-252	-8.1	
III	Central Himalayas	9	Middle Rongbu[72]	28°03´	85°50´	85.4	22.4	N/NW	Central Himalayas	1966-2001	-315	-8.8	-6.3
		10	East Rongbu[72]	28°03´	85°57´	46.3	12.8	NW	Central Himalayas	1966-2001	-198	-5.5	
		11	Kangwure*	28°28´	85°49´	1.9	3.1	NE	Central Himalayas	1976-2007	-294	-9.2	
		12	Dasuopu*	28°25´	85°41´	43.98	14.3	NE	Central Himalayas	1968-2007	-166	-4.1	
		13	Qiangyong*	28°51´	90°13´	7.98	5.5	N	Central Himalayas	1975-2001	-66	-2.4	
		14	Rikha Samba[73]	28°50´	83°31´	4.62	-	-	Nepal Himalayas	1974-1994	-200	-10	
		15	AX010[74]	27°42´	86°34´	0.38	1.7	E/SE	Nepal Himalayas	1978-1999	-150	-6.9	

		16	Yala[75]	28°14′	85°37′	1.88	-	-	Nepal Himalayas	1987-1996	-86	-3.9	
IV	West Himalayas	17	Dokriani[76]	30°50′	78°50′	7	5.5	W	Garhwal Himalayas	1962-1995	-550	-16.6	-16.6
		18	Pindari[77]	30°15′	80°02′	-	5	SW	Kumaun Himalayas	1958-2007	-323	-6.5	
		19	Samudra Tapu[78]	32°30′	77°30′	73	17.7	E	Himachal Pradesh	1962-2000	-741	-19.5	
		20	Chhota Shigri[78]	32°10′	77°31′	15.7	9	N	Himachal Pradesh	1963-2003	-995	-23.7	
		21	Naimona'nyi*	30°27′	81°20′	7.8	7.7	N	West Himalayas	1976-2006	-155	-5	
		22	Milam[79]	30°26′	80°03′	37	16.7	SE	Kumaon Himalayas	1954-2003	-1328	-26.6	
		23	Shaune Garang[80]	30°50′	78°46′	5.6	6.1	N	Garhwal Himalayas	1962-1999	-1500	-40.5	
		24	Tipra Bank[81]	30°52′	78°52′	7.4	-	-	Garhwal Himalayas	1962-2008	-535	-13.4	
		25	Dunagiri[81]	30°54′	78°51′	2.56	-	-	Garhwal Himalayas	1992-1997	-15	-3	
		26	Satopanth[81]	30°56′	78°53′	12	-	-	Garhwal Himalayas	1962-2005	-1157	-26.9	
		27	Chorabari[81]	30°56′	78°53′	6.9	-	-	Garhwal Himalayas	1962-2007	-237	-5.2	
		28	No.13 Glacier[82]	33°39′	76°21′	-	14.7	-	Between Nun Kun Massif and Zanskar Massif in Greater Himalaya Range in Zanskar, southern ladakh	1975-2003	24	0.8	
		29	Drang Drung[82] (No.11)	33°47′	76°19′	-	23.5	-		1975-2003	-224	-7.7	
		30	No.10 Glacier[82]	33°50′	76°18′	-	9.99	-		1975-2003	-1786	-61.6	
		31	No.9 Glacier[82]	33°55′	76°12′	-	14.45	-		1975-2003	-813	-28	

		32	No.8 Glacier[82]	33°46′	76°07′	-	6.98	-		1975-2003	-16	-0.6	
		33	No.7 Glacier[82]	33°46′	76°08′	-	7.5	-		1975-2003	-229	-7.9	
		34	No.4 Glacier[82]	33°55′	76°17′	-	6.6	-		1975-2003	-745	-25.7	
		35	Parkachik (No.2)[82]	33°53′	76°10′	-	12.9	-		1979-2004	91	3.6	
		36	Gangotri[83]	30°50′	79°10′	37.8	8.1	SE	Garhwal Himalayas	1971-2004	-565	-17.15	
		37	Maztag Ata*	38°14′	75°03′	1	1.8	W	Maztag Ata	2002-2010	-13.6	-1.7	
		38	Baltoro[84]	35°50′	76°30′	1500	60	-	Karakoram	1985-2004	32	1.6	
		39	Raikot[85]	35°15′	74°55′	39	15	-	Nanga Parbat region	1954-2007	178	3.3	
		40	Siachen[86]	35°30′	77°00′	987.1	70	NW-SE	Karakorum Mts	1958-2005	0	0	
		41	5Y654D42[87]	35°53′	76°13′	97.8	29.4	NE		1976-2000	-478	-19.1	
V	Pamir regions	42	5Y654D48[87]	35°58′	76°18′	10.2	6.1	NE		1976-2000	2050	82	-0.9
		43	5Y654D53[87]	36°09′	76°01′	158.11	42	NE/E		1968-2000	0	0	
		44	5Y654D77[87]	36°07′	76°18′	8.79	5.3	NE	Muztag Ata and Konggur Mts.	1968-2000	910	27.6	
		45	5Y654D78[87]	36°07′	76°18′	1.5	2.8	NE		1968-2000	140	4.3	
		46	5Y654D97[87]	36°11′	76°08′	15.79	10.7	NE		1968-2000	1998	60.5	
		47	5Y654C81[87]	35°34′	77°25′	32.6	10	NE		1976-2000	0	0	
		48	5Y654C92[87]	35°34′	77°20′	42.14	14.5	N/NW		1976-2000	0	0	

		49	5Y654C116[87]	35°34′	77°13′	105.6	20.8	N/NW		1976-2000	0	0	
		50	5Y654C128[87]	35°37′	76°06′	124.5	28	NE/NW		1976-2000	0	0	
		51	5Y654C145[87]	35°39′	76°55′	83.5	27.8	NW		1976-2000	0	0	
		52	5Y654C163[87]	35°49′	76°38′	119.8	26	NE		1976-2000	0	0	
		53	5Y653K72[87]	35°31′	77°25′	70.7	20.7	SE/NE		1976-2000	0	0	
		54	5Y653Q185[87]	36°04′	76°48′	2.45	4.4	SE		1976-2000	-278	-11.1	
		55	5Y663E14[87]	38°15′	75°06′	14.6	8.6	W/NW		1963-2001	1758	-45	
		56	5Y663E1[87]	38°19′	75°07′	12.12	8.6	N/W		1963-2001	-758	-19.4	
		57	5Y663E8[87]	38°18′	75°05′	8.91	9.4	W		1963-2001	437	11.2	
		58	5Y663D87[87]	38°14′	75°10′	86.5	20.7	E/NE		1963-2001	-226	-5.8	
		59	5Y663B7[87]	38°26′	75°18′	-	6.5	-		1963-2001	-669	-17	
		60	5Y662D35[87]	38°32′	75°19′	103.17	21	SE/E	Karakorum Mts	1964-2001	-1832	-48	
		61	5Y656I27[87]	38°12′	75°12′	7.41	6.5	SW		1976-2001	940	37	
		62	5Y656I22[87]	38°12′	75°12′	1.98	2.1	SW		1976-2001	1410	56.4	
		63	5Y663D24[87]	38°22′	75°21′	5.91	6	SW		1963-2001	-514	-13	
		64	5Y663D36[87]	38°15′	75°27′	11.08	7	NE/NW		1963-2001	1130	29	
		65	5Y663B25[87]	38°37′	75°17′	128.15	20.3	N		1963-2001	0	0	
		66	5Y641F49[88]	35°25′	81°24′	42.33	13.1	NE	West Kunlun Mts	1970-2001	141	4.4	
		67	5Y641F70[88]	35°27′	81°16′	30.09	14.2	NE		1970-2001	-790	-24.7	

		68	5Y641F73[88]	35°29´	81°41´	23.5	14.9	N/NE		1970-2001	446	13.9	
		69	5Y641H67[88]	35°33´	80°35´	41.7	15.1	N/NW		1970-2001	-1431	-44.7	
		70	5Y641F46[88]	35°23´	81°31´	92.8	18.5	NE/N		1970-2001	-616	-19.3	
		71	5Y641H74[88]	35°33´	80°29´	131.8	18.5	NE		1970-2001	-511	-16	
		72	5Y641G38[88]	35°30´	81°52´	90.8	19	N		1970-2001	-903	-28.2	
		73	5Y641F98[88]	35°30´	81°07´	64.27	20	NW		1970-2001	-1176	-36.8	
		74	5Y641G55[88] (Kunlun)	35°26´	80°47´	200	23.6	NE		1970-2001	875	27.3	
		75	5Y641F85[88]	35°28´	81°12´	84.3	26.1	NE/N		1970-2001	-1146	-35.8	
		76	5Y641F63[88] (Yulong)	35°24´	81°18´	139.07	30.9	NE/NW		1970-2001	522	16.3	
		77	5Y641G23 [88] (Duofeng)	35°25´	80°58´	251.7	31	NE		1970-2001	-883	-27.6	
VI	Tanggula	78	Xiao Dongkemadi*	33°10´	92°08´	1.8	2.8	S/SW	Inner TP	1992-2002	-38	-3.4	-2
		79	Malan*	35°50´	90°47´	37.8	8.1	SE		1970-2000	-31	-1	
		80	Purogangri*	33°57´	89°06´	18.5	9.1	SW		1974-2000	-46	-1.7	
VII	Qilian	81	Laohu No.12[89]	39°27´	96°32´	21.9	10.1	N/NW	Qilian Mts	1977-2005	-157	-5.4	-4.2
		82	Qiyi*	39°15´	97°45´	2.8	3.8	N		1970-2008	-114	-3	

Supplementary Table S5 Detailed information on the glaciers for recent mass balance measurement in the TP and surroundings

Region	Glacier number	Glaciers	Latitude (N)	Longitude (E)	Area (km^2)	Maximum elevation (m a.s.l.)	Minimum elevation (m a.s.l.)	Length (km)	Orientation	Locations
I	1	Parlung No.10	29°17′	96°54′	2.1	5625	4910	3.5	NE	Southeast TP
	2	Parlung No.12	29°18′	96°54′	0.2	5265	5130	0.6	NE	Southeast TP
	3	Parlung No.94	29°23′	96°59′	2.5	5635	5000	2.9	NW	Southeast TP
	4	Parlung No.390	29°21′	97°01′	0.5	5460	5160	1.2	SE	Southeast TP
II	5	Gurenhekou	30°11′	90°28′	1.4	6040	5525	2.9	SE	Nyainqentanglha Mountain
	6	Zhongxi	30°52′	91°27′	1.6	6210	5376	2.6	N	Nyainqentanglha Mountain
III	7	Kangwure	28°28′	85°49′	1.9	6060	5690	3.1	NE	Central Himalayas
	8	AX010[90]	27°42′	86°34′	0.4	5302	4968	1.7	E/SE	Central Himalayas
	9	Yala[90]	28°14′	85°37′	1.9	5642	5086	1.5	SW	Central Himalayas
IV	10	Naimona'nyi	30°27′	81°20′	7.8	7520	5465	7.7	N	West Himalayas
	11	Hamtah[91]	32°21′	81°22′	-	-	-	-	-	West Himalayas
	12	Chhota Shigri[92]	32°12′	81°30′	15.7	6263	4050	9	N	West Himalayas
V	13	Muztag Ata	38°14′	75°03′	1	5940	5235	1.8	W	West Kunlun Mountain
VI	14	Xiaodongkemadi	33°10′	92°08′	1.8	5926	5380	2.8	S/SW	Tanggula Mountain
VII	15	Qiyi	39°15′	97°45′	2.8	5088	4295	3.8	N	Qilian Mountain

Supplementary Table S6 Recent annual mass balances in different regions in the TP.

Regions	Glaciers	2002/03	2003/04	2004/05	2005/06	2006/07	2007/08	2008/09	2009/10	Average	Regional average
I	Parlung No.10	-	-	-	-675	-283	-593	-1575	-	-781	-1105
	Parlung No.12	-	-	-	-1449	-1112	-1410	-2476	-2046	-1698	
	Parlung No.94	-	-	-	-913	-254	-1079	-2018	-347	-922	
	Parlung No.390	-	-	-	-	-170	-1250	-1673	-982	-1019	
II	Gurenhekou	-	-	-	-319	-196	497	-839	-703	-312	-418
	Zhongxi	-	-	-	-	-	264	-1045	-789	-523	
III	Kangwure	-	-	-	-1023	-392	-487	-1092	-300	-660	-757
	AX010[90]*				-810				-	-810	
	Yala[90]*				-800				-	-800	
IV	Naimona'nyi	-	-	-	-658		-718	-472	-276	-556	-908
	Hamtah[91]	-	-1857	-1856	-790	-	-	-	-	-1501	
	Chhota Shigri[92]	-1400	-1227	144	-1400	-980	-930	130	330	-667	
V	Muztag Ata	-	-	-	-237	956	79	220		248	248
VI	Xiaodongkemadi	-	-	-	-917	-591	-80	-91	-1066	-549	-549
VII	Qiyi	-	-	-	-955	-513	-105	-74	-648	-459	-459

*The average mass balances AX010 (1999-2008) and Yala Glacier (1996-2009) were taken to represent the recent mass balance since 2002/03. The red color numbers for the Kangwure Glacier were reconstructed following the method in Section 3.2.

Supplementary Table S7 Mass balance of Long-time series for the Qiyi, Xiaodongkemadi and Kangwure Glaciers in the TP.

Years	Qiyi	Xiaodongkemadi	Kangwure
1975	35	-	-
1976	384	-	-
1977	350	-	-
1978	-1	-	-
1979	241	-	-
1980	130	-	-
1981	-51	-	-
1982	197	-	-
1983	292	-	-
1984	226	-	-
1985	-31	-	-
1986	-165	-	-
1987	38	-	-
1988	-49	-	-
1989	-205	525	-
1990	183	45	-
1991	-405	-180	-
1992	132	375	-250
1993	441	210	-640
1994	-285	-510	-484
1995	-273	-570	-460
1996	-615	-495	-308
1997	-293	345	-251
1998	46	-690	-507
1999	-778	-315	-397
2000	-612	-90	-229
2001	-666	-195	-685
2002	-810	-583	-496
2003	-361	4	-574
2004	-634	-153	-479
2005	-476	-177	-728
2006	-955	-917	-1023
2007	-513	-591	-392
2008	-105	-80	-487
2009	-74	-91	-1092
2010	-648	-1066	-300

* The red color numbers are the reconstructed mass balance.

Supplementary Figures

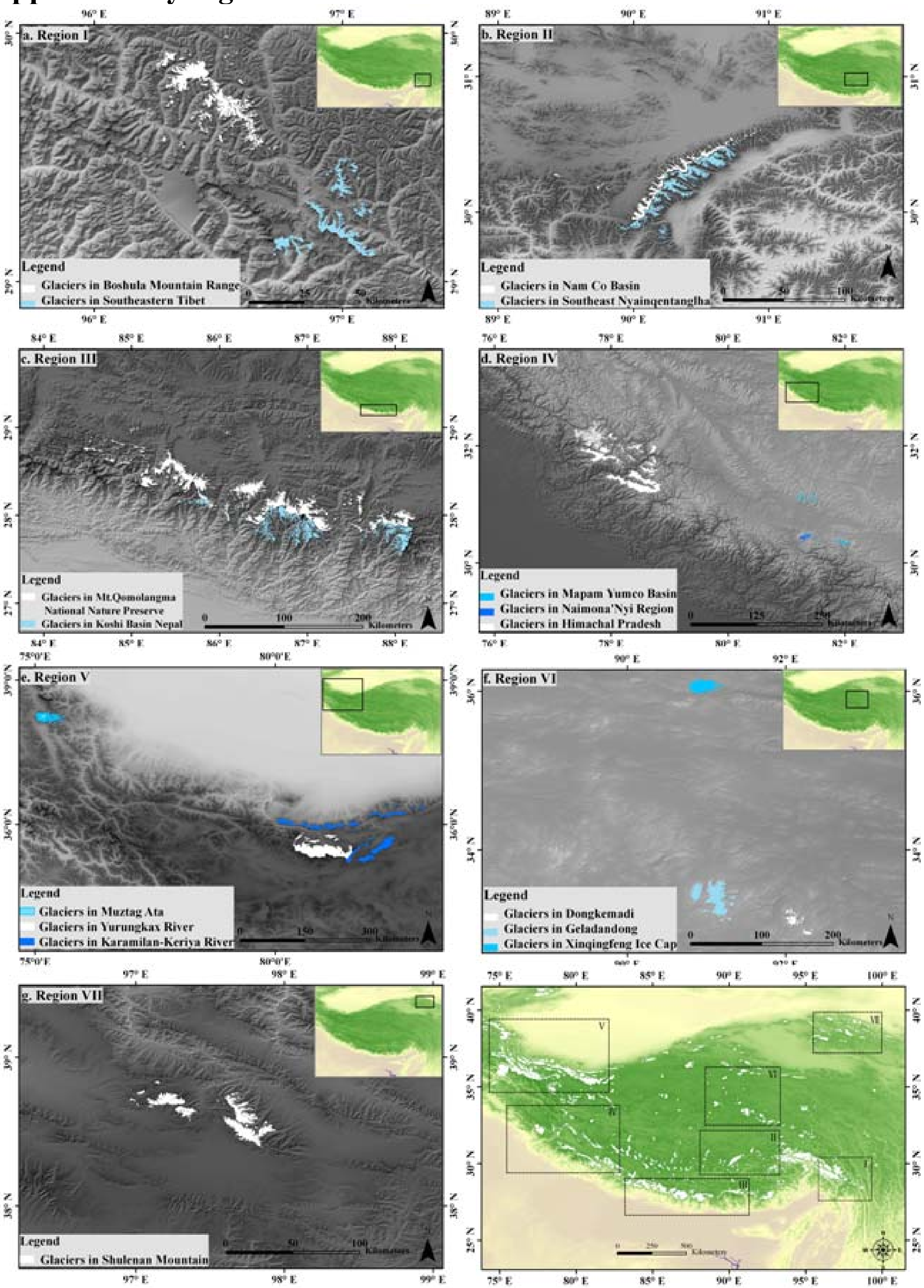

Supplementary Figure S1. The distribution of glaciers for analyzing area reduction studies in the seven regions.

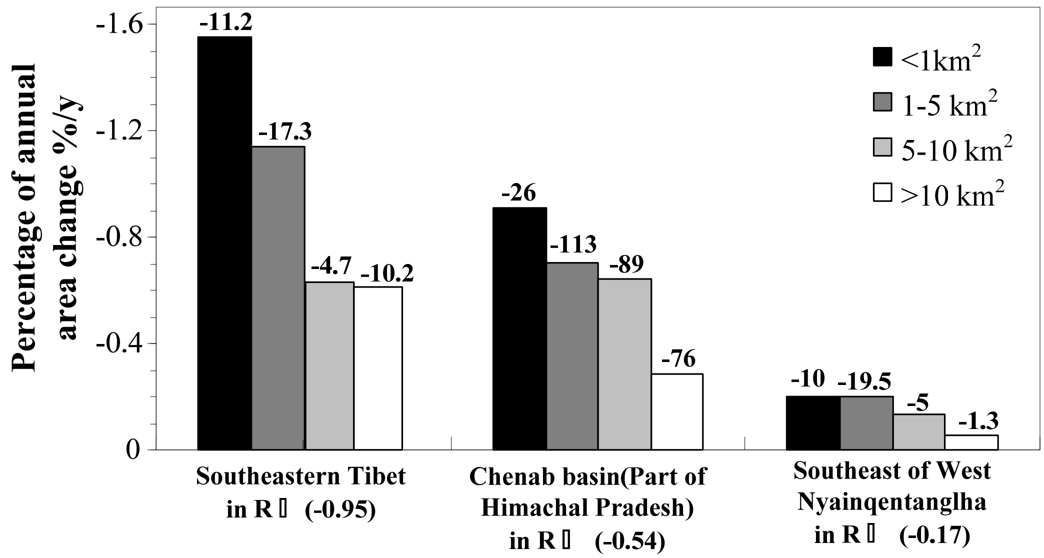

Supplementary Figure S2 Comparison of the change of glacier with different sizes in different regions. The absolute area changes (km^2) are shown on top of each column. The number in the parentheses is the percentage of annual area change of this region.

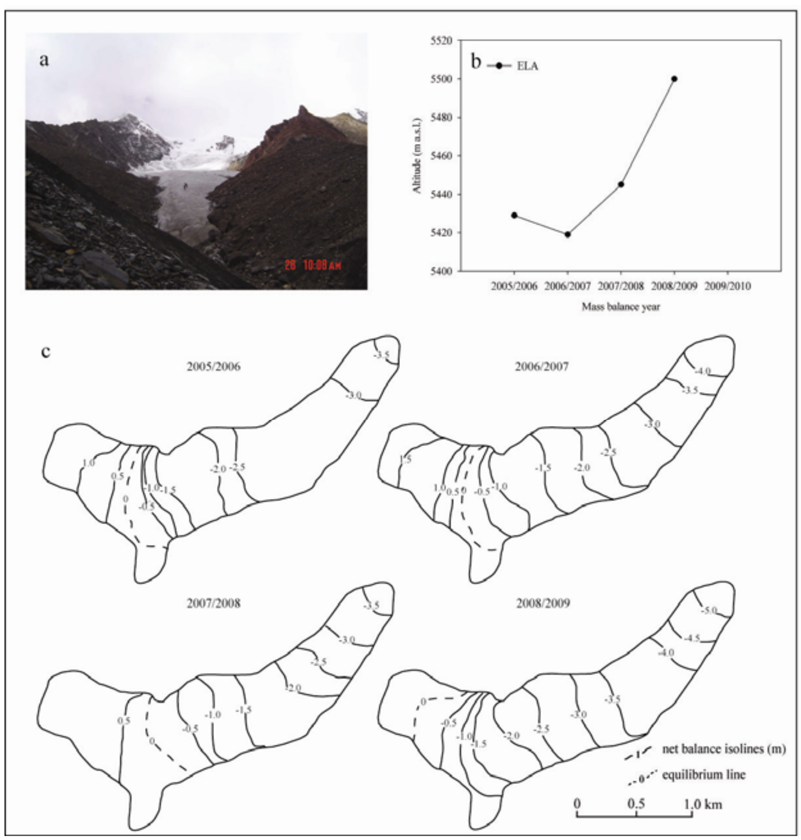

Supplementary Figure S3 The Parlung No. 10 Glacier. a) Photo of the Parlung No.10 Glacier, b) variation of ELAs and c) spatial mass balance distribution in past four balance years

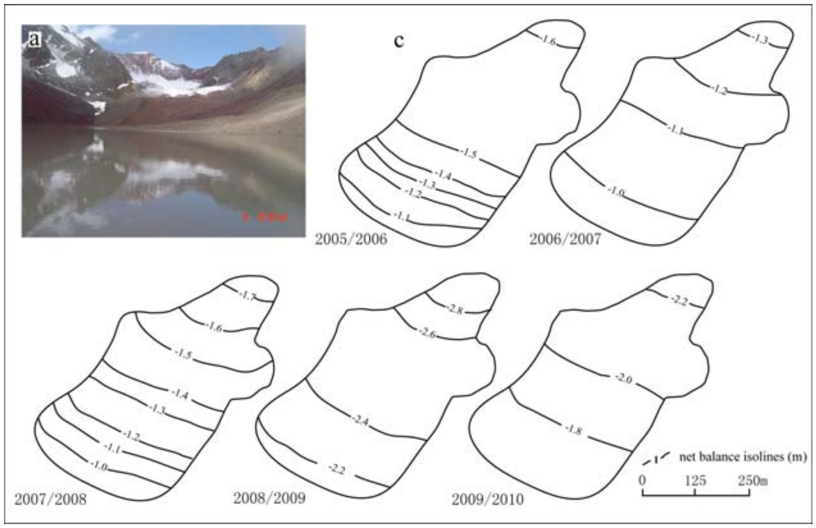

Supplementary Figure S4 The Parlung No. 12 Glacier. a) Photo of the Parlung No.12 Glacier, c) spatial mass balance distribution in past five balance years

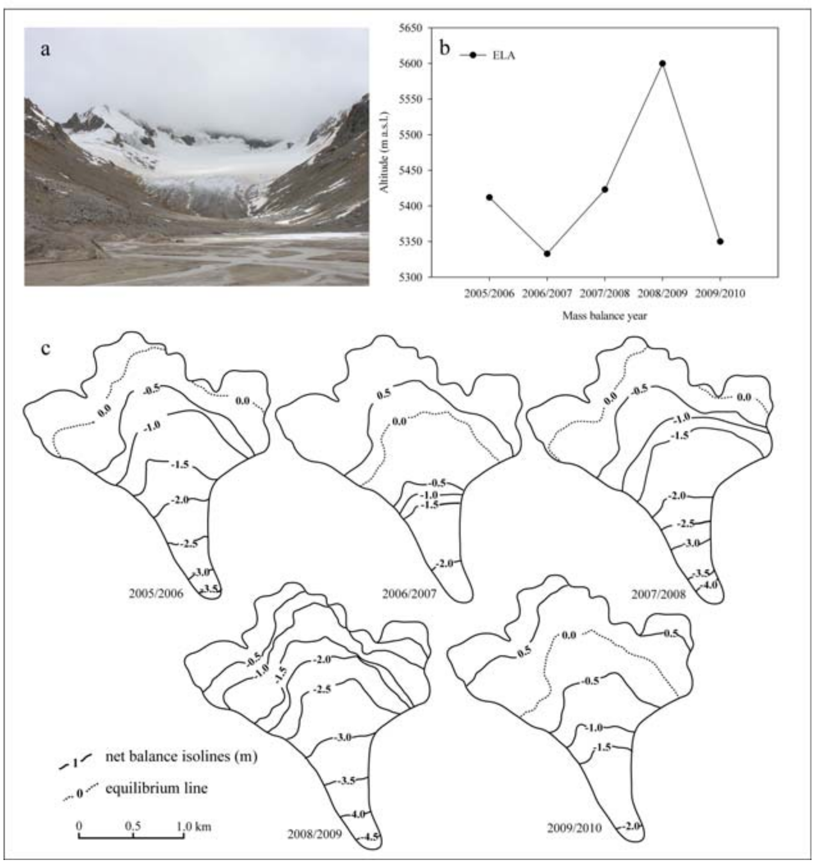

Supplementary Figure S5 The Parlung No. 94 Glacier. a) Photo of the Parlung No.94 Glacier, b) variation of ELAs and c) spatial mass balance distribution in past five balance years

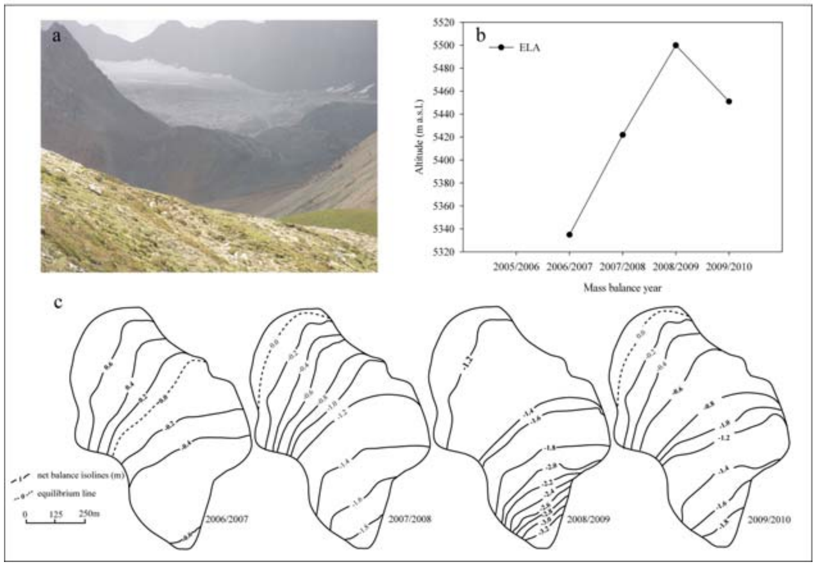

Supplementary Figure S6 The Parlung No. 390 Glacier. a) Photo of the Parlung No.390 Glacier, b) variation of ELAs and c) spatial mass balance distribution in past four balance years

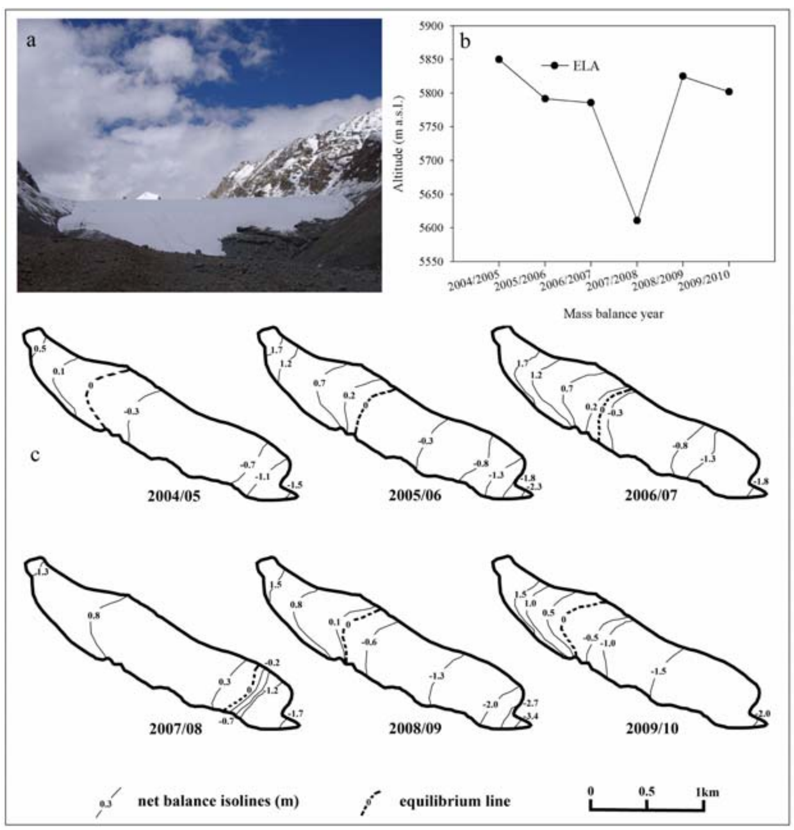

Supplementary Figure S7 The Gurenhekou Glacier. a) Photo of the Gurenhekou Glacier, b) variation of ELAs and c) spatial mass balance distribution in past six balance years

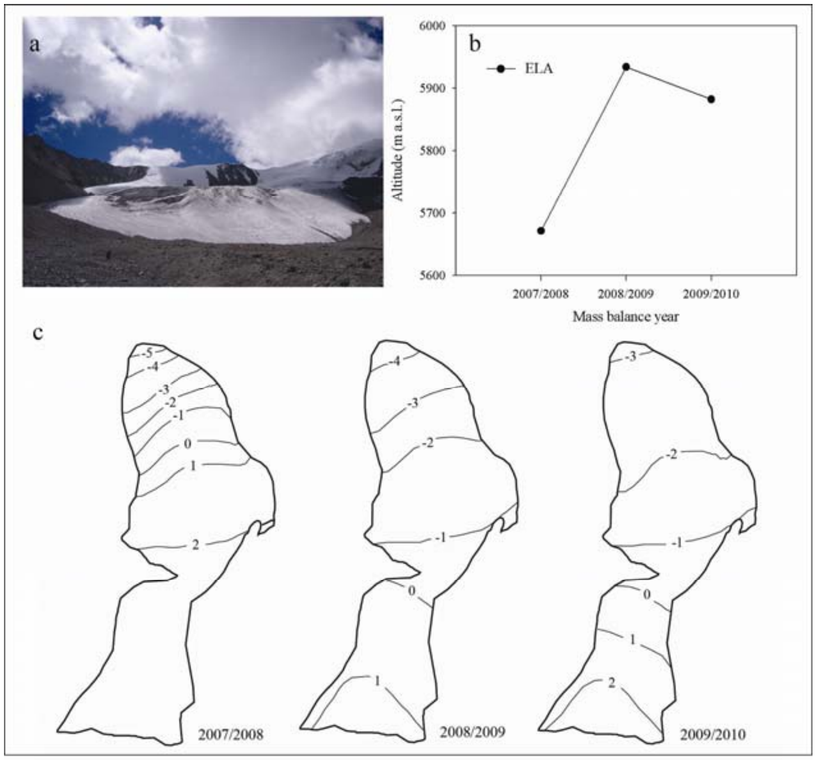

Supplementary Figure S8 The Zhongxi Glacier. a) Photo of the Zhongxi Glacier, b) variation of ELAs and c) spatial mass balance distribution in past three balance years

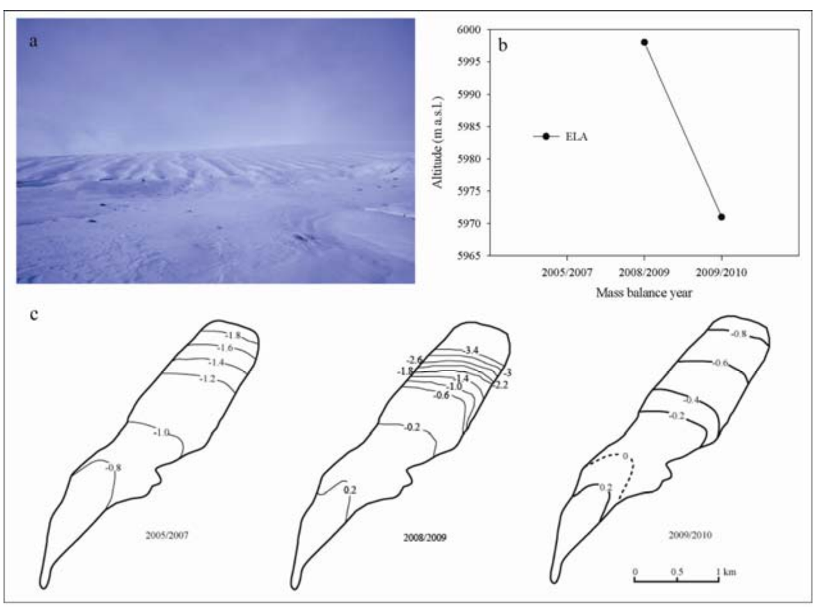

Supplementary Figure S9 The Kangwure Glacier. a) Photo of the Kangwure Glacier, b) variation of ELAs and c) spatial mass balance distribution in past three balance years

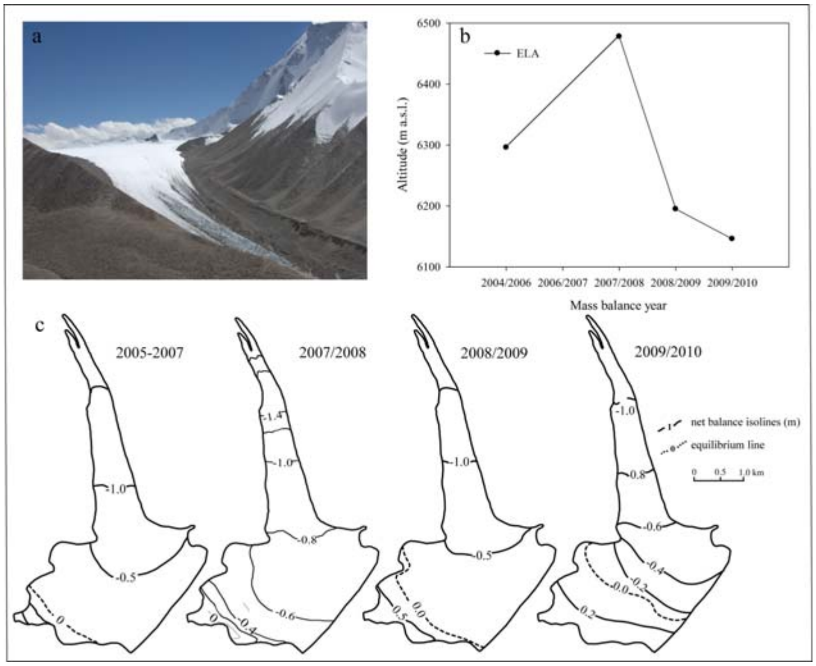

Supplementary Figure S10 The Naimona'nyi Glacier. a) Photo of the Naimona'nyi Glacier, b) variation of ELAs and c) spatial mass balance distribution

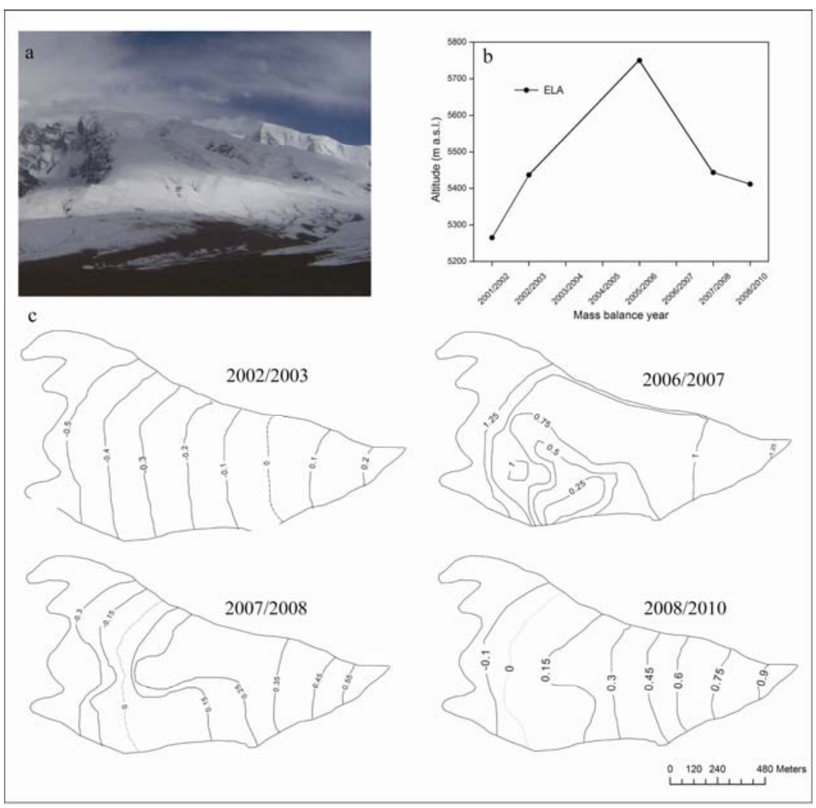

Supplementary Figure S11 The Muztag Ata Glacier. a) Photo of the Muztag Ata Glacier, b) variation of ELAs and c) spatial mass balance distribution

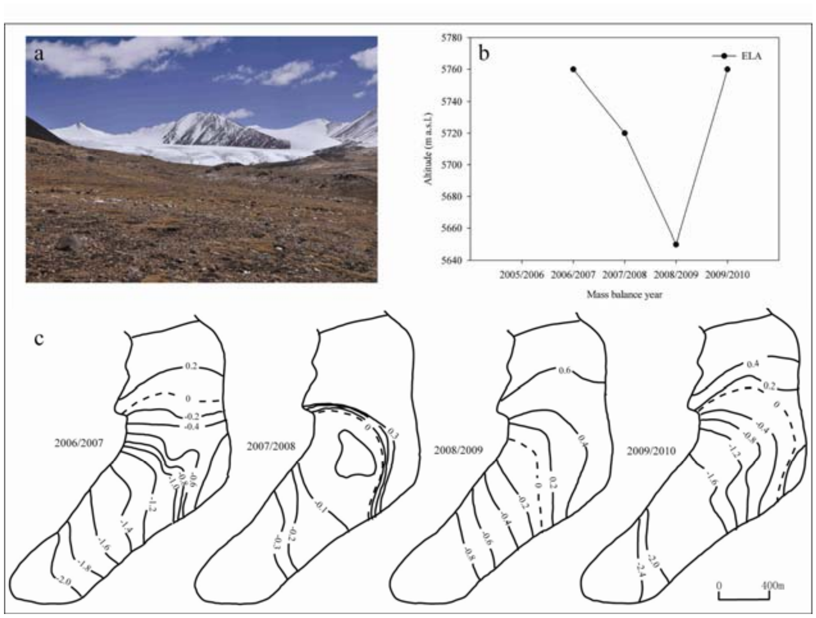

Supplementary Figure S12 The Xiaodongkemadi Glacier. a) Photo of the Xiaodongkemadi Glacier, b) variation of ELAs and c) spatial mass balance distribution in past four balance years

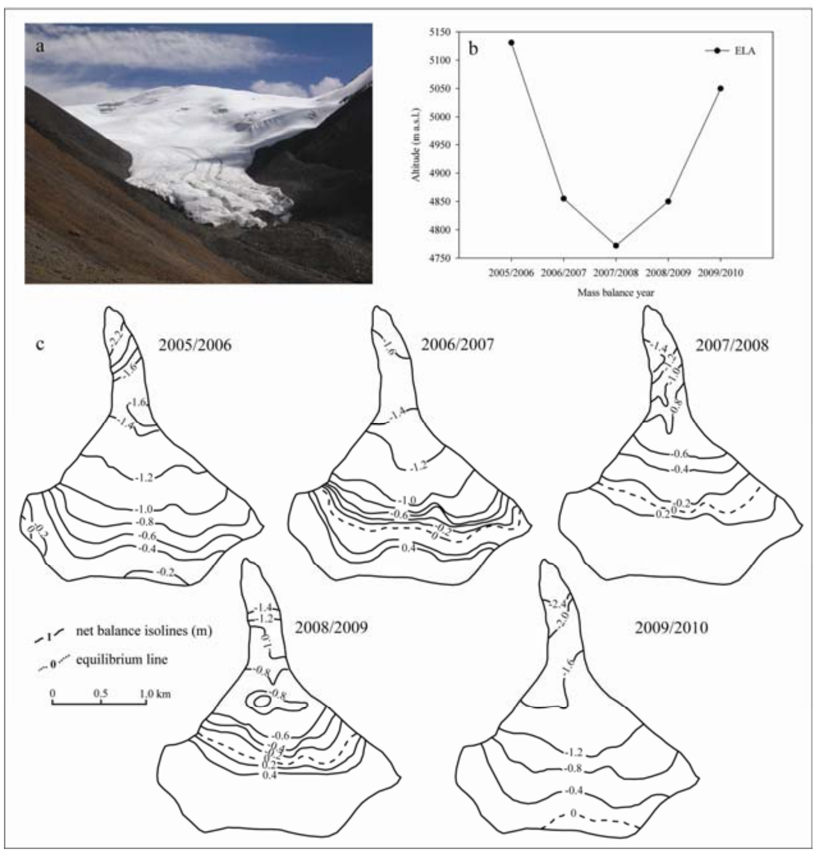

Supplementary Figure S13 The Qiyi Glacier. a) Photo of the Qiyi Glacier, b) variation of ELAs and c) spatial mass balance distribution in past four balance years

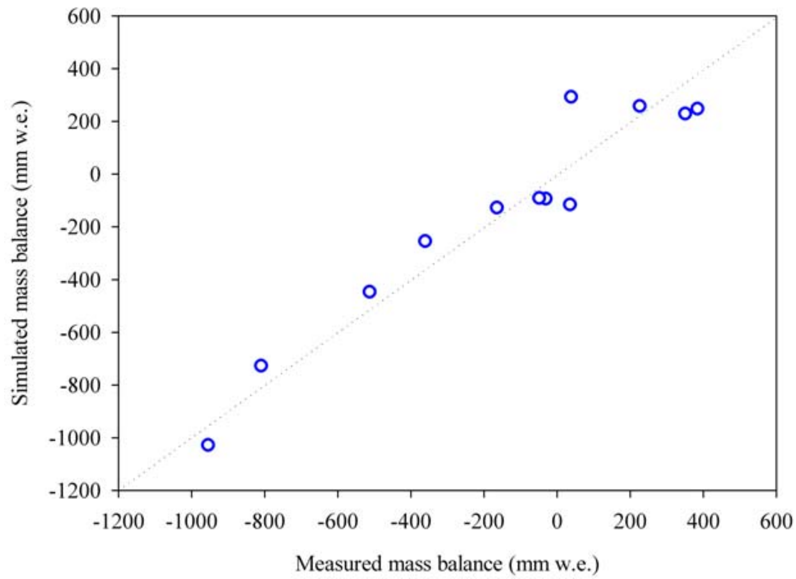

Supplementary Figure S14 Comparison between measured and simulated mass balance for the Qiyi Glacier.

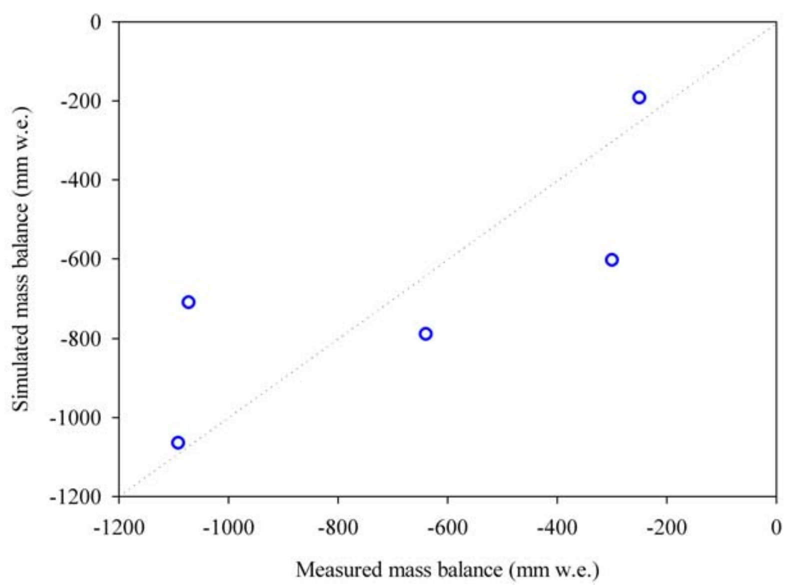

Supplementary Figure S15 Comparison between measured and simulated mass balances for the Kangwure Glacier.

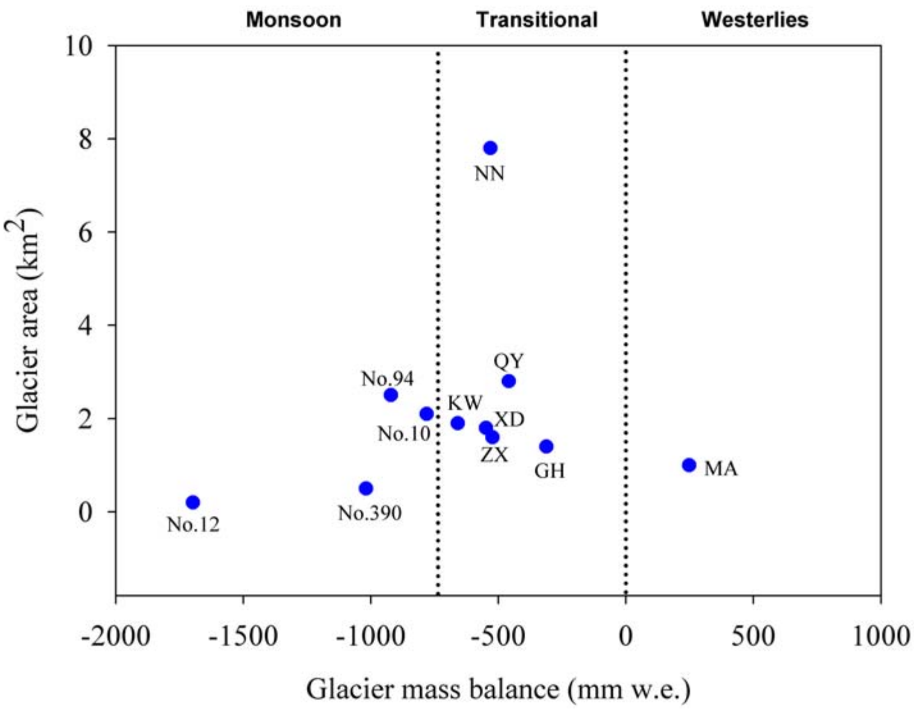

Supplementary Figure S16 Distinctive features of glacial mass balance under different climate dominances. (No. 10, 12, 94, 390-Parlung No. 10, 12, 94, 390; NN-Naimona'nyi; QY-Qiyi; KW-Kangwure; XD-Xiaodongkemadi; ZX-Zhongxi; GH-Gurenhekou; MA-Muztag Ata)

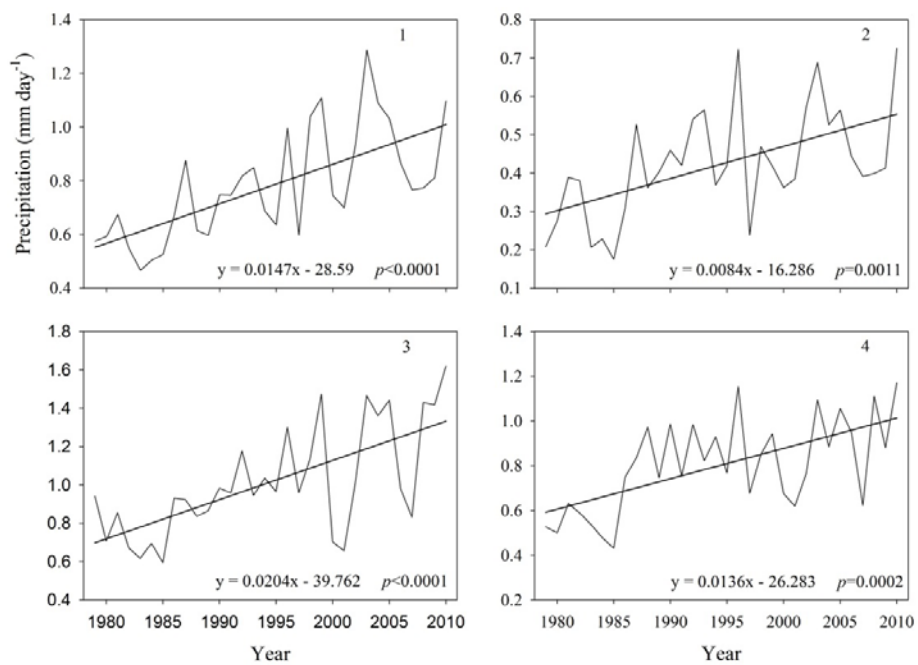

Supplementary Figure S17 The linear trends of GPCP precipitation (mm day^{-1}) for 1979−2010 from the grids numbered as 1-4 in Figure S4g. All the positive trends are statistically significant at the 99% confidence level using the Mann-Kendall test.

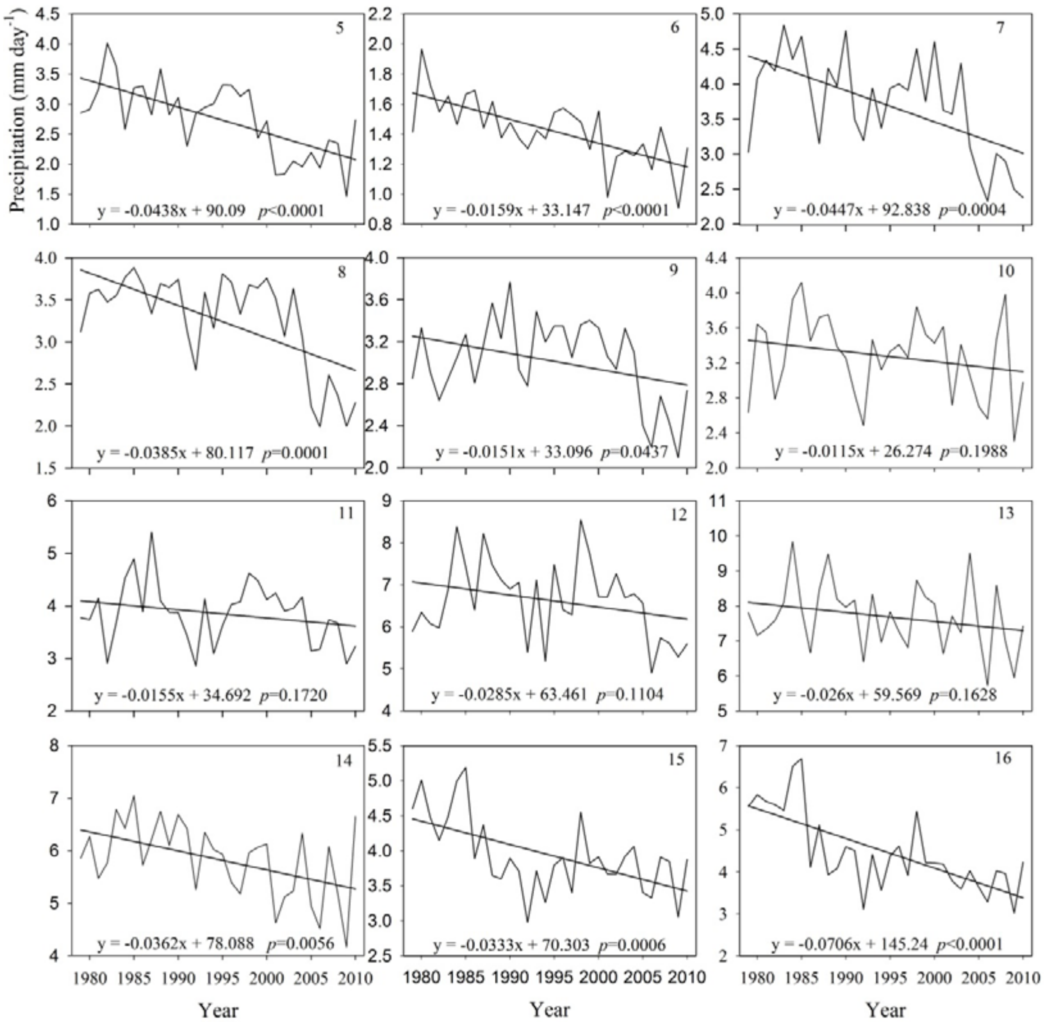

Supplementary Figure S18 The linear trends of GPCP precipitation (mm day^{-1}) for 1979−2010 from the grids numbered as 5-16 in Figure S4g. The native trends for No.5−8 and No.14−16 are statistically significant at the 99% confidence level using the Mann-Kendall test.

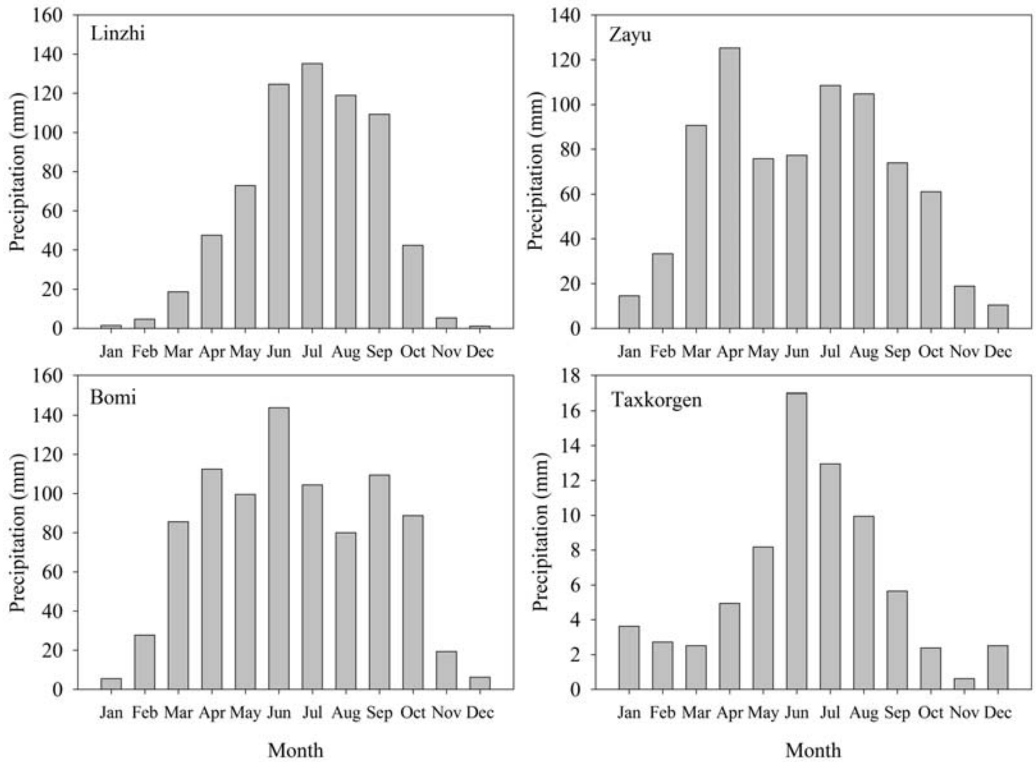

Supplementary Figure S19 The monthly mean precipitation at the meteorological stations of Linzhi, Zayu, Bomi and Taxkorgan during 1970-2009. The precipitation at all the four stations shows a strong seasonality characterized by high precipitation in the summer and low precipitation in the winter.

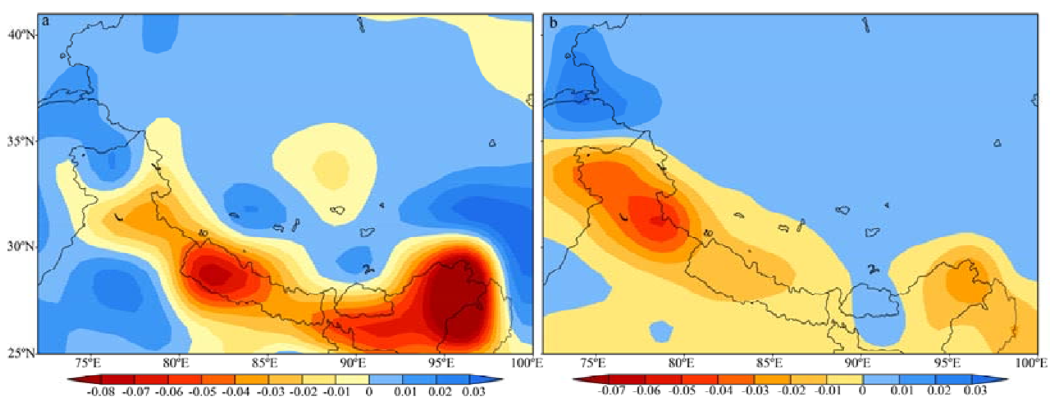

Supplementary Figure S20 The spatial feature of GPCP precipitation (mm day^{-1}) trend in the summer (a) and winter (b) seasons in the TP and surroundings during 1979-2010. Similar to the annual spatial trends in Figure 4a in the text, the summer and winter spatial trends demonstrate decreasing precipitation in the eastern Himalayas and increasing precipitation in the eastern Pamir regions, with more intensive decreasing in the summer in the Indian monsoon-dominated Himalayas and more intensive increasing in the winter in the westerlies-dominated Pamir regions.

Supplementary References

(*for references 1 to 30 see main text*)

31. Shi, Y. *et al*. *Concise Glacier Inventory of China* (in Chinese) (Shanghai Popular Science Press, Shanghai, China, 2008).
32. Dyurgerov, M. B. *Glacier mass balance and regime: Data of measurements and analysis, INSTAAR Occas*. Pap. 55, edited by M. Meier and R. Armstrong, Inst. of Arct. and Alp. Res., Boulder, Colo (2000).
33. Shi, Y. & Liu, S. Estimation on the response of glaciers in China to the global warming in the 21st century. *Chin. Sci. Bull.* **45**, 668-672 (2000).
34. Yao, T. *et al*. Recent glacial retreat in High Asia in China and its impact on water resource in Northwest China. *Sci. China Ser. D* **47**(12), 1065-1075 (2004).
35. Yao, T. *et al*. Glacial distribution and mass balance in the Yarlung Zangbo River and its influence on lakes. *Chin. Sci. Bull.* **55**(20), 2072-2078 (2010).
36. Yang, W. *et al*. Characteristics of recent temperate glacier fluctuations in the Parlung Zangbo River basin, southeast Tibetan Plateau. *Chin. Sci. Bull.* **55**(20), 2097-2102 (2010).
37. Ma, L., Tian, L., Pu, J. & Wang, P. Recent area and ice volume change of Kangwure Glacier in the middle of Himalayas. *Chin. Sci. Bull.* **55**(20), 2088-2096 (2010).
38. Jiang, X., Wang, N., He, J., Wu, X. & Song, G. A distributed surface energy and mass balance model and its application to a mountain glacier in China. *Chin. Sci. Bull.* **55**(20), 2079-2087 (2010).
39. Wang, N., He, J., Pu, J., Jiang, X. & Jing, Z. Variations in equilibrium line altitude of the Qiyi Glacier, Qilian Mountains, over the past 50 years. *Chin. Sci. Bull.* **55**(33), 3810-3817 (2010).
40. Yang, W. *et al*. Quick ice mass loss and abrupt retreat of the maritime glaciers in the Kangri Karpo Mountains, southeast Tibetan Plateau. *Chin. Sci. Bull.* **53**, 2547-2551(2008).
41. Xin, X., Yao, T., Ye, Q., Guo, L. & Yan, W. Study of the Fluctuations of Glaciers and Lakes around the Ranwu Lake of Southeast Tibetan Plateau using Remote Sensing. *J. Glaciol. Geocryol.* **31**(1), 19-26 (2009).
42. Li, Z., Yao, T., Ye, Q., Tian, L. & Wang, W. Glaciers in the upstream Manla Reservoir in the Nianchu River basin, Tibet: shrinkage and impact. *J. Glaciol. Geocryol.* **32**(4), 650-658 (2010).
43. Pu, J., Yao, T., Wang, N., Su, Z. & Shen, Y. Fluctuations of the glaciers on the Qinghai-Tibetan Plateau during the past century. *J. Glaciol. Geocryol.* **26**(5), 517-522 (2004).
44. Ren, J. *et al*. Glacier variations and climate warming and drying in the central Himalayas. *Chin. Sci. Bull.* **49**, 65-69 (2004).
45. Qin, D. *Map of Glacial Resource in the Himalayas* (in Chinese) (Science Press, Beijing, China, 1999).
46. Liu, S., *et al*. Glacier Variations since the Early 20th Century in the Gangrigabu Range,

Southeast Tibetan Plateau. *J. Glaciol. Geocryol.* **27**, 55-63 (2005). (In Chinese)

47. Jin, R., Che, T., Li, X. & Wu, L. Glacier Variation in the Pumqu Basin Derived from Remote Sensing Data and GIS Technique. *J. Glaciol. Geocryol.* **26**, 261-266 (2004). (In Chinese)
48. Liu, C., Kang, E., Liu, S., Chen, J. & Liu, Z. Study on the glacier variation and its runoff responses in the arid region of Northwest China. *Sci. China Ser. D* **42**(supp), 64-71 (1999).
49. Su, Z. & Shi, Y. Response of monsoonal temperate glaciers in China to global warming since the Little Ice Age. *J. Glaciol. Geocryol.* **22**(3), 223-229 (2000).
50. Shi, Y. *et al*. Glaciers and related environments in China. Science Press, Beijing, 2008.
51. Yang, W., Yao, T., Xu, B. & Zhou, H. Influence of supraglacial debris on the summer ablation and mass balance in the 24K Glacier, southeastern Tibetan Plateau. *Geogr. Ann. Ser. A-Phys. Geogr.* 92, 353-360 (2010).
52. Bolch, T., Pieczonka, T. & Benn, D. I. Multi-decadal mass loss of glaciers in the Everest area (Nepal Himalaya) derived from stereo imagery. *Cryosphere*, **5**, 349-358 (2011).
53. Fujita, K. & Ageta, Y. Effect of summer accumulation on glacier mass balance on the Tibetan Plateau revealed by mass-balance model. *J. Glaciol.* **46**, 244-252 (2000).
54. Kang, S. *et al*. Review of climate and cryospheric change in the Tibetan Plateau. *Environ. Res. Lett.* **5**, doi:10.1088/1748-9326/5/1/015101 (2010).
55. Andreassen, L. M., Paul, F., Kääb, A. & Hausberg, J. E. Landsat-derived glacier inventory for Jotunheimen, Norway, and deduced glacier changes since the 1930s. *Cryosphere.* **2**, 131-145 (2008).
56. Paul, F., Kääb, A., Maisch, M., Kellenberger, T., & Haeberli, W., The new remote-sensing-derived Swiss glacier inventory: I. Methods. *Ann. Glaciol.* **34**, 355-361(2002).
57. Bolch, T. & Kamp, U. Glacier mapping in high mountains using DEMs, Landsat and ASTER data. In Kaufmann, V. and W. Sulzer, eds. Proceedings of the 8th International Symposium on High Mountain Remote Sensing Cartography. Graz, Karl Franzens University, 13-24 (2006). (Grazer Schriften der Geographie und Raumforschung 41)
58. Bhambri, R., Bolch, T., Chaujar, R.K. & Kulshreshtha, S. C. Glacier changes in the Garhwal Himalaya, India, from 1968 to 2006 based on remote sensing. *J. Glaciol.* **57**(203), 543-556 (2011).
59. Bolch, T. *et al*. A glacier inventory for the western Nyainqêntanglha Range and the Nam Co Basin, Tibet, and glacier changes 1976-2009. *Cryosphere* **4**, 419-433 (2010).
60. Shangguan, D. *et al*. Variation of glaciers in the Western Nyainqentanglha Range of Tibetan Plateau during 1970-2000. *J. Glaciol. Geocryol.* **30**(2), 204-210 (2008). (In Chinese)
61. Nie, Y., Zhang, Y., Liu, L. & Zhang, J. Monitoring glacier change based on remote sensing in the Mt. Qomolangma National Nature Preserve, 1976-2006. *Acta. Geogr. Sin.* **65**(1), 13-28 (2010). (In Chinese)
62. Guo, L. Ye, Q., Yao, T., Chen. F. & Cheng, W. The glacial landforms and the changes of

glacier and lake area in the Mapam Yumco basin in Tibetan Plateau based on GIS. *J. Glaciol. Geocryol.* **29**(4), 517-524 (2007). (In Chinese)

63. Ye, Q., Chen, F., Stein, A. & Zhongz. Use of a multi-temporal grid method to analyze changes in glacier coverage in the Tibetan Plateau. *Prog. Nat. Sci*. **19**, 861-872 (2009).
64. Kulkarni, A. *et al.* Glacial retreat in Himalaya using Indian Remote Sensing satellite data. *Curr. Sci*. **92**(1), 69-74 (2007).
65. Cai, D. Ma, J., Nian, Y., Liu, S. & Shangguan D. The study of glacier change using remote sensing in Mt.Muztagta. *J. Lanzhou University (Natural Sciences)* **42**(1), 13-17 (2006). (In Chinese)
66. Shangguan, D., Liu, S., Ding, Y., Ding, L. & Li, G. Glacier changes at the head of Yurungkax River in the west Kunlun Mountains in the past 32 years. *Acta. Geogr. Sin.* **59**(6), 855-862 (2004). (In Chinese)
67. Xu, J. Liu, S., Zhang, S. & Shangguan, D. Glaciers fluctuations in the Karamilan-Keriya River Watershed in the past 30 years. *J. Glaciol. Geocryol.* **28**, 312-318 (2006). (In Chinese)
68. Qiao, C. Remote sensing monitoring of glacier changes in Dongkemadi region of Tanggula Mountain. *J. Anhui Agri. Sci.* **38**(14), 7703-7705 (2010). (In Chinese)
69. Liu, S. *et al*. Variation of glaciers studied on the basis of RS and GIS-A reassessment of the changes of the Xinqingfeng and Malan ice caps in the northern Tibetan Plateau. *J. Glaciol. Geocryol.* **26**(3), 244-252 (2004). (In Chinese)
70. Liu, S. *et al*. Glacier change during the past century in the Gangrigabu mountains, southeast Qinghai-Xizang (Tibetan) Plateau, China. *Ann. Glaciol.* **43**, 187-193 (2006).
71. Kang, S. *et al*. Glacier retreating dramatically on the Mt. Nyainqentanglha during the last 40 years. *J. Glaciol. Geocryol.* **29**, 869-873 (2007). (In Chinese)
72. Ren, J., Jing, Z., Pu, J. & Qin, X. Glacier variations and climate change in the central Himalaya over the past few decades. *Ann. Glaciol.* **43**, 218-222 (2006).
73. Fujita, K., Nakawo, M., Fujii, Y. & Paudyal, P. Change in glaciers in Hidden Valley, Mukut Himal, Nepal Himalayas, from 1974 to 1994. *J. Glaciol.* **43**, 583-588 (1997).
74. Fujita, K., Kadota, T., Rana, B. Kayastha, R. B. & Agata, Y. Shrinkage of Glacier AX010 in Shorong region, Nepal Himalayas in the 1990s. *Bull. Glaciol. Res.* **18**, 51-54 (2001).
75. Fujita, K., Takeuchi, N. & Seko, K. Glaciological observations of Yala Glacier in Langtang Valley, Nepal Himalayas, 1994 and 1996. *Bull. Glaciol. Res.* **16**, 75-81 (1998).
76. Dobhal, D., Gergan, J.T. & Thayyen, R.J. Recession and morphogeometrical changes of Dokriani glacier (1962-1995) Garhwal Himalaya, India. *Curr. Sci.* **86**, 692-696 (2004).
77. Rameshwar, B., Agarwal, K. K., Sheikh, N. A. & Purnima, S. Is the recessional pattern of Himalayan glaciers suggestive of anthropogenically induced global warming? *Arab. J. Geosci*. **4**, 1087-1093 (2011).
78. Kulkarni, A. V., Dhar, S., Rathore, B. P., Babu, G. R. K. & Kalia, R. Recession of Samudra Tapu glacier, Chandra River basin, Himachal Pradesh. *J. Indian Soc. Remote Sens.* **34**, 39-46

(2006).

79. Raj, K. Recession and reconstruction of Milam Glacier, Kumaon Himalaya, observed with satellite imagery. *Curr. Sci.* **100**, 1420-1425 (2011).

80. Philip, G. & Prasad, M. Mapping repeated surges and retread of glaciers using IRS-1C/1D data: a case study of Shaune Garang glacier, northwestern Himalaya. *Int. J. Appl. Earth Observ. Geoinf.* **6**,127-141 (2004).

81. Dobhal, D. Climate change and Himalayan glaciers: Observations and facts. South Asia Media Briefing Workshop on Climate Change. 24-25, November, 2010.

82. Kamp, U., Byrne, M. & Bolch, T. Glacier fluctuations between 1975 and 2008 in the Greater Himalaya Range of Zanskar, Southern Ladakh. *J. Mt. Sci.* **8**, 374-389 (2011).

83. Kumar, K. Dumka, R.K., Miral, M.S., Satyal, G.S. & Pant, M. Estimation of retreat rate of Gangotri glacier using rapid static and kinematic GPS survey. *Curr. Sci.* **94**(2), 258-261 (2008).

84. Mayer, C.,Lambrecht, A., Belò, M., Smiraglia, C. & Diolaiuti, G. Glaciological characteristics of the ablation zone of Baltoro glacier, Karakoram, Pakistan. *Ann. Glaciol.* **43**(1), 123-131 (2006).

85. Schmidt, S. & Nüsser, M. Fluctuations of Raikot Glacier during the past 70 years: a case study from the Nanga Parbat massif, north Pakistan. *J. Glaciol.* **55**, 949-959 (2009).

86. Raina, V. & Sangewar, C. Siachen Glacier of Karakoram mountains, Ladakh–its secular retreat. *J. Geol. Soc. India.* **70**, 11-16 (2007).

87. Shangguan, D., Liu, S., Ding, Y. & Ding, L. Monitoring results of glacier change in China Karakorum and Muztag Ata-Konggur Mountains by remote sensing. *J. Glaciol. Geocryol.* **26**, 374-375 (2004). (In Chinese).

88. Shangguan, D., Liu, S., Ding, Y., Ding, L. & Li, G. Glacier changes at the head of Yrungkax river in the West Kunlun Mountains in the past 32 years. *Acta. Geogr. Sin.* **59**, 855-862 (2004). (In Chinese)

89. Du, W., Qin, X., Liu, Y. & Wang, X. Variation of the Laohugou Glacier No.12 in the Qilian Mountains. *J. Glaciol. Geocryol.* **30**(3), 373-379 (2008). (In Chinese)

90. Fujita, K. & Nuimura, T. Spatially heterogeneous wastage of Himalayan glaciers. *Proc. Natl. Acad. Sci. USA.* **108**, 14011-14014 (2011).

91. Haeberli, W., Gärtner-Roer, I., Hoelzle, M., Paul, F. & Zemp, M. G. Glacier mass balance bulletin no. 10 (2006-2007). *IAHS (ICSI), Zürich* (2009).

92. Azam, M.F. *et al*. From balance to imbalance: a shift in the dynamic behaviour of Chhota Shigri glacier, western Himalaya, India. *J. Glaciol.* **58**, 315-324 (2012).

93. Kehrwald, N. *et al*. Mass loss on Himalayan glacier endangers water resources. *Geophys. Res. Lett.* **35**, doi:10.1029/2008GL035556 (2008).

94. Wang, N., He, J., Pu, J., Jiang, X. & Jing, Z. Variations in equilibrium line altitude of the Qiyi Glacier, Qilian Mountains, over the past 50 years. *Chin. Sci. Bull.* **55**, 3810-3817 (2010).

95. Liu, S., Xie, Z., Song, G., Ma, L. & Ageta, Y. Mass balance of Kangwure (flat-top) Glacier on the north side of Mt. Xixiabangma, China. *Bull. Glaciol. Res*. **14**, 37-43 (1996).

96. Yao, T.,

97. Frauenfeld, O. W., T. Zhang, and M. C. Serreze (2005), Climate change and variability using European Centre for Medium-Range Weather Forecasts reanalysis (ERA-40) temperatures on the Tibetian Plateau, Journal of Geophysical Reseach, 110, doi:10.1029/2004JD005230.

98. You, Q., et al. (2010), Relationship between temperature trend magnitude, elevation and mean temperature in the Tibetan Plateau from homogenized surface stations and reanalysis data, Global and Planetary Change, 71, 124-133.

99. Adler, R. *et al.* The Version 2 Global Precipitation Climatology Project (GPCP) Monthly Precipitation Analysis (1979-Present). *J. Hydrometeor.* **4**, 1147-1167 (2003).